DOI: 10.21062/mft.2025.027 http://www.journalmt.com

Process Optimisation for Orthogonal Testing of Shot Peening Based on Secondary Development of ABAQUS

Anheng Wang (0009-0009-3555-164X)[1*], Shangqi Duan (0009-0005-0075-726X)[1], Wei Zhang (0009-0000-1133-4119)[1], Fan Li (0009-0005-8369-4347)[2]
[1]School of Mechanical and Automotive Engineering, Anhui Polytechnic University, Wuhu 241000, China
[2]School of Mechanical Engineering, Anhui Institute of Information Technology, Wuhu 241000, China
[*]Email: wahazf@ahpu.edu.cn

This study focuses on 7B50 aluminium alloy with the aim of reducing the pre-treatment and post-treatment times of shot peening models. Optimal combination of peening solutions can be obtained by comparing and analyzing different process parameters. Pre-processing is implemented through GUI interactive interface, while post-processing is developed using Python for secondary development in ABAQUS. Orthogonal test method is used for post-processing analysis of shot peening simulations under different process conditions. The weighted composite scoring method is used to evaluate the results and determine the depth of the residual compressive stress layer on the surface of the workpiece, the surface residual compressive stress, and the extreme deviation of the maximum residual compressive stress value after shot peening. Finally, the comprehensive influence of shot peening process parameters such as impact speed, projectile diameter and impact angle is determined. The optimal combination of shot peening process parameters is analyzed and verified through simulation.

Keywords: ABAQUS secondary development, Orthogonal test method, Shot peening modelling, Surface texture, Residual compressive stresses

1 Introduction

Shot peening is a crucial surface strengthening technique that uses high-speed projectile to impact on the workpiece surface, achieving plastic deformation and grain refinement on the surface layer of the material, thereby forming a certain thickness of the strengthened layer [1]. This technique has a significant impact on enhancing the fatigue strength, wear resistance, fatigue resistance and corrosion resistance of the components [2]. Due to its easy operation, simple process, low cost and ability to handle different shapes of workpiece surfaces, it has been extensively used in the domains of national defense, aviation, transportation and so on. Shot peening is a cold treatment procedure process commonly used to enhance the fatigue characteristics of metal components that withstand high-stress circumstances during long-term service, such as aircraft engine compressor blades, parts of the fuselage structure, components of the automotive powertrain, and other fatigue related properties [3]. Shot peening treatment on the surface of the component will form a layer of residual compressive stress. The compressive stress on the surface can greatly increase the fatigue strength of the component, thereby extending its fatigue life. Meanwhile, as a cold processing method, shot peening can increase the dislocation density on the surface of the component, refined the surface grain, play a role in cold hardening, and suppress the growth of fatigue cracks. In addition, shot peening can transfer the fatigue source from the surface of the component to a position beneath the surface. The fatigue limit resulting from the fatigue source below the surface layer is 1.3 to 1.4 times that of the surface layer. The effectiveness of shot peening is affected by many factors, including peening speed, angle and shot diameter size. If only relying on human efforts to process the test results and analyze them to deduce a rational combination of experimental parameters, it would only result in significant consumption of manpower and materials and may lead to errors [4].

Nowadays, many scholars have conducted extensive numerical simulation analysis on the changes of shot peening parameters and the simulation of shot peening models. Various technologies and methods are put forward to focus on exploring a series of key issues such as the specific impact and potential patterns of shot peening parameter changes on model simulation. Xie et al. [5] established a shot peening finite element model to study the residual stress distribution on the surface layer of Ti-6Al-4V. In this analysis, the simulation results revealed that the compressive residual stress is generated in the surface layer, and the maximum value is in the subsurface layer, which provides an important theoretical basis for process optimization. Zhang et al. [6] conducted numerical simulation on the shot peening of 17Cr2Ni2MoVNb steel. The results showed that different peening residuals

can change the surface compressive residual stress distribution of the steel. Moreover, the surface compressive residual stress and the maximum compressive residual stress depth are proportional to the peening rate. In addition, the maximum compressive residual stress depth increased as the coverage rate increased gradually. Gariépy et al. [7] experimentally analyzed the properties of AA2024-T351 aluminum alloy after repeated random impacts. The results showed that in the post expansion state, the surface planes of this material are characterized by non-uniformity in terms of residual stresses, local mechanical properties, roughness, and surface damage due to non-uniform conditions caused by the initial crystallography and processing. Wu et al. [8] simulated the effect of coverage on the residual stress and roughness of 18CrNiMo7-6 steel, and found that a high surface coverage can improve the synthetic effect of sprayed materials. However, current focus is on the change of a single parameter, lacking in-depth investigation and comprehensive analysis of the combined effects of multiple parameters, which may affect the understanding of material properties and the determination of application directions. Li et al. [9] showed that the residual compressive stresses generated on the surface of alloys using shot peening can improve the fatigue properties of alloys.

ABAQUS based-secondary development has been widely used in many fields [10-11]. Gao et al. [12] proposed a dynamic constitutive model prediction model embedded in ABAQUS software by using the secondary development, and verified its correctness. This provides a practical tool for finite element analysis of material molding. Qiang et al. [13] proposed an integrated constitutive model and verified the proposed numerical model by experimental. The model can effectively describe the stress-strain relationship of Fe-SMA under static loading with high accuracy.

Taking the 7B50 aluminium alloy as the research object, based on the secondary development program of Python in ABAQUS, a finite element model of random projectile impact on the target material is constructed. Based on the orthogonal test method, the effects of three process parameters, impact speed, projectile diameter and impact angle, on the residual stress and roughness are investigated. The optimal combination of process parameters is obtained to enhance the shot peening accuracy of the 7B50 aluminum alloy, and achieve the optimal shot peening effect.

2 Python in ABAQUS secondary development and applications

ABAQUS is finite element analysis software with numerous features. Python, as an efficient scripting language, is extensively used in the secondary development of ABAQUS [14]. Therefore, model modifications can be realized using script files written in Python, which call a graphical user interface tool to execute ABAQUS script commands. Files with the extension ".py" written in Python can be executed through the ABAQUS Python interface, and then the two can be connected for pre-processing and subsequent post-processing of the stochastic blast model [15].

In a given relationship, there is a unique way of interacting with the data, and the two are closely connected in this way, as shown in Fig. 1. Users can input commands as ".rpy" files via the graphical interface (GUI), command line interface (CLI), and scripts. These commands are read by the Python interpreter and transferred to the ABAQUS kernel for execution. In ABAQUS, the commands are transformed into INP files, which are then analyzed by the ABAQUS explicit solver, ultimately generating post-processing output files.

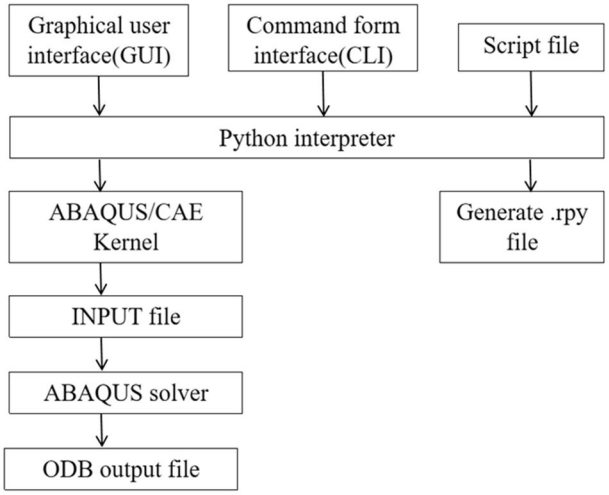

Fig. 1 *The communication of Python with ABAQUS*

3 GUI interactive interface design

The design of the interactive GUI interface takes on a crucial role. Users can use MATLAB software for modelling via the interactive interface, wherein the GUI interactive interface cannot only enhance the user experience, but also considerably augment the functionality and use of the software [16]. The designed graphical user interface (GUI) is programmed using the tkinter library function in the Python language, which can be used to generate various GUI interfaces. To simulate users' requirements for different Shot peening parameters, several main parameter input fields are generated in the interactive interface. Given the large amount of code involved in designing a GUI interface, it would be too complicated to explain each line of code. In this case, only some of the most important core parts are selected for in-depth analysis. The selected code includes the overall

framework of the GUI interface, presentation of each window creation, configuration of the two functional buttons of reset and run, as well as the task submission for pre-processing. Upon the integration of the above components, the GUI interface of this thesis will be prepared for normal operation and application.

```
01 root = tk.Tk()root.title("Parameter input interface")
02 label1 = tk.Label(root, text = "Random shot peening model parameter inter
face")
03 label2 = tk.Label(root, text = "Target size", foreground = 'black', font = 2
0)
04 label3 = tk.Label(root, text = "Edge length:"))
05 label4 = tk.Label(root, text = "Thickness:", foreground = 'red', font =10)
06 label5 = tk.Label(root, text = "Shot peening parameters", font = 20)
07 label3 = tk.Label(root,text = " Speed :", foreground = 'red', font = 10)
08 with open(' paras.py','w',encoding = 'utf -8') as f : f.write(string)messagebox.
button = tk.Button(root, text = "Run",command = generation)
```

(Code 1)

In the above code, the first line is known, and the second line sets the stochastic shot peening model parameter input interface to the header, which is important for subsequent operations. The code from lines 3 to 7 is for generating the panel that displays only the values of the five parameters, rather than all of them. The values entered in the GUI interactive interface are assigned to the script file; line 8 generates the script file with the modified parameters and saves it in the same folder.

3.1 Interactive interface function

The Random Shot Peening model constitutes a multi-variable and multi-constraint design specification. To enhance the efficiency of modelling and simulation in a practical and effective way, human labor has been reduced. The tkinter library is used to design a customized shot peening interactive GUI, allowing users to accurately input test parameters and generate basic scripts for the ABAQUS secondary development process. In this script file, we have clearly defined the parameters that need to be changed, so that users can easily modify and recall undefined parameters. The function of each section can be observed in the script file of the GUI backend, providing users with a deeper comprehension of the internal code. Based on the parameters entered in the interactive interface, just click on the "Generate" button, the script will automatically run in the background, quickly generate a script file with the ".py" extension. This script file is crucial for further development of ABAQUS.

3.2 Introduction to the interactive interface

The GUI interactive interface is designed, as shown in Fig. 2. There are eight main variables in this interactive interface: the length and thickness of the target square, target and projectile properties: density, Young's modulus, Poisson's ratio, and shot peening parameters: shot peening speed, shot size and shot peening angle. There are also two function buttons for reset and run. The interactive interface includes numerical input fields for target size, shot peening parameters and material properties, which can be customized to meet users' requirements. The interactive interface can be automated to quickly generate the required ".py" script files, which provides a basis for post-processing of the model.

Fig. 2 *GUI interactive interface*

4 Creation of Random Shot Simulation Model Scripts

To improve the flexibility and scalability of the script, a modular design is used to separate and explain different functional modules. The Stochastic Shot Peening Simulation Model is composed of eight modules: Parts, Properties, Assemblies, Steps, Interactions, Loads, Meshes, and Jobs. To avoid wasting time due to errors during the script generation process of the final blast simulation model file, it is recommended to conduct sufficient testing and verification work after creating each module to ensure the correctness and reliability of the script [17-18]. During the testing process, multiple test parameters are used to cover various possible scenarios and boundary conditions. The generated script has been optimized and improved to enhance testing efficiency and ensure that the final simulation model achieves the expected results. The subsequent simulation analysis has received strong support.

4.1 Model pre-processing script building

4.1.1 Setting material properties

The code aims to assign the material parameters of the ball and target. First, two material property libraries, "Mat ball" and "Mat plat", are generated, and then we can utilize the GUI interactive interface to enter the material parameters of the ball and target.

```
Sphere Properties
mdb.models['Model-1'].Material('Mat_ball')
mdb.models['Model-1'].materials['Mat_ball'].Density()
mdb.models['Model-1'].materials['Mat_ball'].Elastic(table=(E1, U1),)
mdb.models['Model-1'].HomogeneousSolidSection()
Target Properties
mdb.models['Model-1'].Material('Mat_plat')
mdb.models['Model-1'].materials['Mat_plat'].Density()
mdb.models['Model-1'].materials['Mat_plat'].Elastic(table=(E2, U2))
mdb.models['Model-1'].materials['Mat_plat'].Plastic()
```

(Code 2)

4.1.2 Create an analysis step

The code is divided into three analysis steps: Initial, Step-1 and quadBulkViscosity and the response time interval for the Step-1 analysis step is set to 0.0003. The grid size of the quadBulkViscosity projectile mesh for the analysis step is set to 0.04.

```
mdb.models['Model-1'].ExplicitDynamicsStep(name='Step-1', previous=
'Initial', timePeriod=3e-4, quadBulkViscosity=0.04)
session.viewports['Viewport:1'].assemblyDisplay.setValues(step='Step-1')
```

(Code 3)

4.1.3 Creating boundaries

This code aims to establish boundary conditions of the ball, which is constrained within the peening area. The target has complete constraints around and on the bottom surface, thereby simulating the actual constraint state of the peening target. Therefore, it can better achieve the realism of simulating the impact process.

```
mdb.models['Model-1'].DisplacementBC(name='BC-'+str(i),
createStepName='Initial'
region=region, u1=UNSET, u2=UNSET, u3=UNSET, ur2=SET,
ur3=SET, amplitude=UNSET, distributionType=UNIFORM, fieldName='',local
Csys=None)
```

(Code 4)

4.1.4 Meshing

```
p = mdb.models['Model-1'].parts['plat']
p.seedEdgeByBias(biasMethod=SINGLE, end1Edges=pickedEdges1,
end2Edges=pickedEdges2, minSize=0.04, maxSize=0.4, constraint=FINER)
p = mdb.models['Model-1'].parts['plat']
p.generateMesh()
```

(Code 5)

4.1.5 Submission of mandates

This code is used to generate a Job 1 model file, submit the job, and input the generated file into the ABAQUS solver. That is to say, all preprocessing steps for building the script file of the random shot peening model have been completed so far, as shown in Fig. 3, which displays the generated random shot peening model.

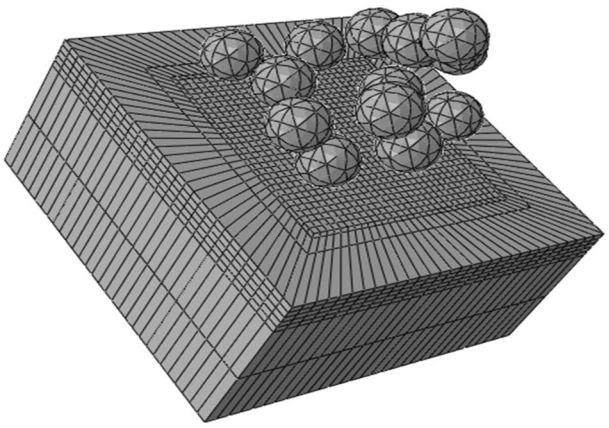

Fig. 3 *Model diagram of the pre-processing results*

```
mdb.jobs['Job-1'].submit(consistencyChecking=OFF, datacheckJob=True)
session.mdbData.summary()
```

(Code 6)

4.2 Shot peening simulation post-treatment analysis

Post-processing can be carried out by clicking on the monitor in the Job module to view the results. The pre-processing script written here can only achieve parametric modeling and submit calculations. The calculation results such as equivalent force cloud, target surface deformation, and roughness can be viewed in the visualization module, as shown in Fig. 4.

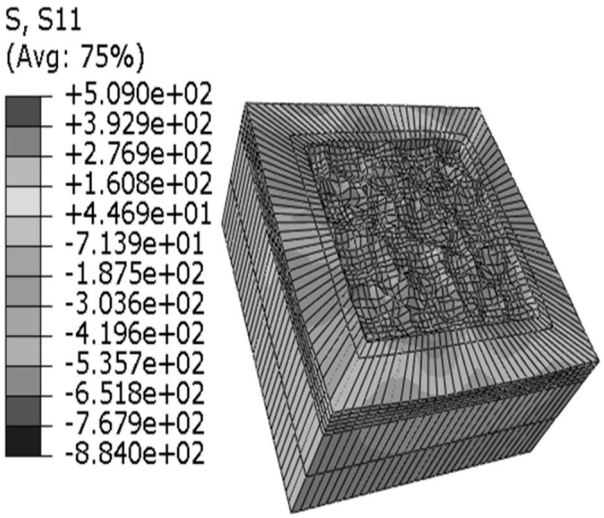

Fig. 4 *Model post-processing diagram*

5 Random shot peening simulation

A GUI interface is designed using the orthogonal test method to input various shot peening parameters. Subsequently, the corresponding shot peening model is generated using the running script, enabling a comprehensive and in-depth analysis of the simulation test.

5.1 Shot peening parameterization of finite element models

The Johnson-Cook model is used in the simulation process to characterize the strain-hardening and strain-rate-hardening behavior of the target material in single and multi-shot models. In addition, the model is used to investigate the response and changes in the material during shot peening. The expressions are as follows:

$$\sigma = (A + B\varepsilon^{n})\left[1 + C\ln\left(\frac{\overline{\varepsilon}}{\overline{\varepsilon}_0}\right)\right]\left[1 - \left(\frac{T - T_0}{T_m - T_0}\right)^{m}\right] \tag{1}$$

Where:
A…The yield strength of the material, MPa;
B…The material parameter, MPa;
C…The strain rate parameter;
n…The hardening parameter;
m…The thermal softening parameter;
σ…The equivalent flow stress;
ε …The equivalent plastic strain (PEEQ);
$\overline{\varepsilon}$ …The equivalent plastic strain;
$\overline{\varepsilon}_0$ …The reference strain rate;
T…The material temperature;
T_m and T_0…The melting point and room temperature of the material, respectively.

The target material is 7B50 aluminium alloy, and the projectile is cast steel shot. The mechanical properties of the target and projectile are shown in Tab. 1. The chemical composition of 7B50 aluminium alloy is shown in Tab. 2.

Tab. 1 *Parameters of mechanical properties of the impacted body and the impacting body*

Making	Densities ϱ/(kg·m⁻³)	Young's modulus E/GPa	Poisson's ratio γ
7B50 aluminium alloy	2830	71	0.33
cast steel shot	5500	210	0.3

Tab. 2 *Chemical composition of 7B50 aluminium alloy (mass fraction %)*

Si	Fe	Zn	Cu	Mn	Mg	Cr	Zr	Al
0.10	0.10	6.48	2.06	0.10	2.24	0.04	0.09	Residuals

Due to the impact of the projectile, the surface of the target undergoes elastic deformation. Therefore, the Johnson-Cook intrinsic model is used and the parameters are obtained from Ref. [19]. To facilitate the study, the sprayed coverage is set at 150 per cent. The dimension of the target is 2 mm x 2 mm x 1 mm, and the mesh density has a notable influence on the analysis results. To improve the accuracy of the calculation results, it is necessary to fully refine the mesh of jet collision region to obtain the residual stress field. Since the center region of the workpiece surface is in contact with the projectile, it is necessary to refine the mesh of the contact region of the workpiece surface [20]. The grid cell dimension of the target is set at 0.04mm, while the projectile grid cell dimension is set as 0.1mm. The cell type is C3D8R, and the analysis step time is set to 3×10^{-4} s. The cell type remains as C3D8R, and the analysis step time is also set to 3×10^{-4} s. The bottom surface of the workpiece uses a fixed displacement boundary, and the spherical center of the pellet is established as the reference point to set the pellet properties.

5.2 Orthogonal test method for shot peening process

The orthogonal test method is capable of determining the optimal combination of shot peening parameters in a minimum number of trials, providing a high reference value for the process. After the simulation test, the results are analyzed with the help of polarity analysis. The role of process parameters on shot peening and the correlation between the parameters are clarified to reach the optimal combination of process parameters. The main parameters affecting the effectiveness of shot peening are identified and used as guidelines for subsequent tests [21].

Shot peening produces large residual compressive stresses on the surface of the workpiece. At the same time, the depth of the residual compressive stress layer is also affected to a certain extent. In view of this, this paper will measure three basic parameters of residual compressive stress, including the depth of the residual compressive stress layer. These three indices will be optimized as a comprehensive score as an evaluation criterion [22]. The way to combine the parameters of shot peening process will be explored to achieve the best results of shot peening.

Under the interactive interface of the graphical user interface (GUI), pre-processing operations are carried out on the shot peening model first. Then, a simulation study is carried out using orthogonal test methods based on the shot peening model. Finally, the simulation results of shot peening are analyzed and processed uniformly to propose the optimal combination of shot peening parameters in the experimental process plan.

6 Orthogonal test analysis of optimal combination of shot peening parameters

6.1 Evaluation indices of shot peening reinforcement

Key indicators for evaluating the peening effect of shot peening are the residual compressive stress on the surface of the workpiece and the depth of the compressive stress layer. A large compressive stress and a deep compressive stress layer have a good peening effect. The residual compressive stress can improve the fatigue strength and corrosion resistance of the workpiece, and the deep compressive stress layer can provide long-lasting protection. When evaluating these two indicators, they should be improved to ensure material strengthening. The specific evaluation indices are defined as the surface residual compressive stress X_1 (σ_s), the depth of the residual compressive stress layer X_2 (d_0), and the maximum residual compressive stress X_3 (σm). The larger the three selected target values, the higher the overall evaluation score will be, and the better the mechanical properties of the surface will be, enabling the fatigue resistance of the workpiece to be effectively enhanced [23].

6.2 Selection of shot peening parameters and simulation of orthogonal tests

More factors would affect the residual stress of shot peening. In this orthogonal test, only three main factors that affect the shot peening are selected.

The three factors are: the shot peening impact speed A ($m.s^{-1}$), the diameter of the projectile B (mm), and the impact angle of the shot peening C (°). To investigate the factors affecting the effectiveness of shot peening, orthogonal test method is used to establish and conduct 9 groups of simulation experiments. The experimental design scheme is shown in Tab. 3.

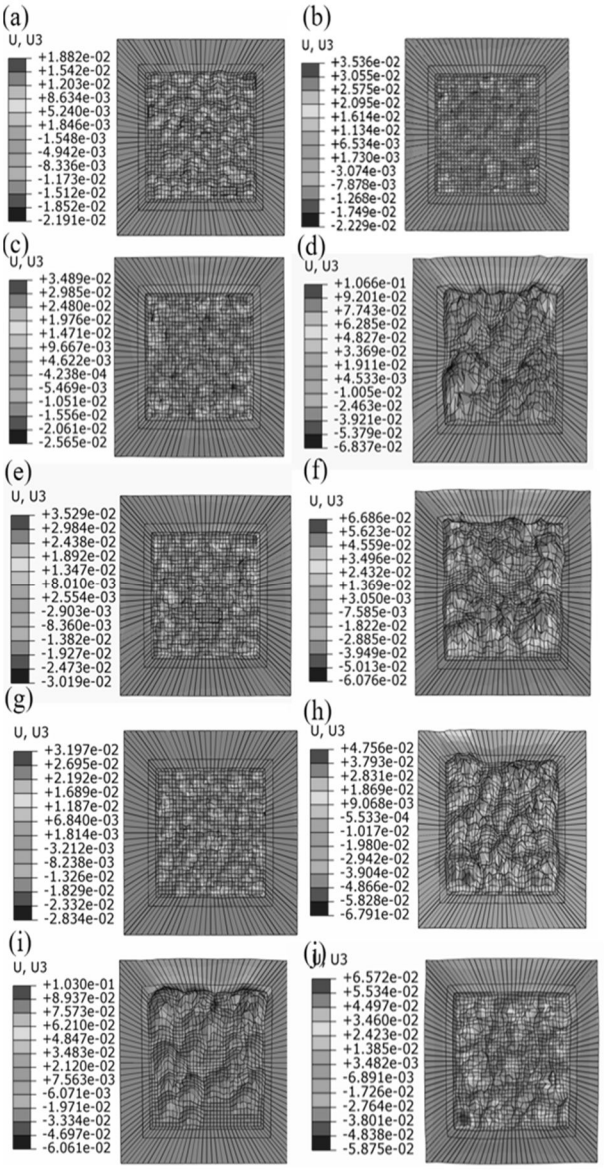

Fig. 5 *Roughness surface topography; Test Group Number: (a)Test 1, (b)Test 2, (c)Test 3, (d)Test 4, (e)Test 5, (f)Test 6, (g)Test 7, (h)Test 8, (i)Test 9 (j) Optimal combination of solutions*

Tab. 3 *Different factors and levels*

Level factors	Levels corresponding to different shot peening parameters		
	Peening impact velocity A ($m.s^{-1}$)	Bullet diameter B (mm)	Angle of Projectile Impact C (°)
Level 1	60	0.3	45
Level 2	80	0.4	60
Level 3	100	0.5	90

As shown in Fig. 5, the particle diameter, shooting speed, and angle have a significant influence on the roughness. When the blasting speed is set at 60 $m.s^{-1}$, and the incidence angles are 45° and 90°in Fig. 5 (a) and Fig. 5 (b) respectively. In Fig. 5 (a), when the incidence angle is 45°, many irregular and relatively large craters are formed on the material surface. In Fig. 5 (b), when the incidence angle is 90°, there is only a large number of uniform small craters that are relatively smooth.

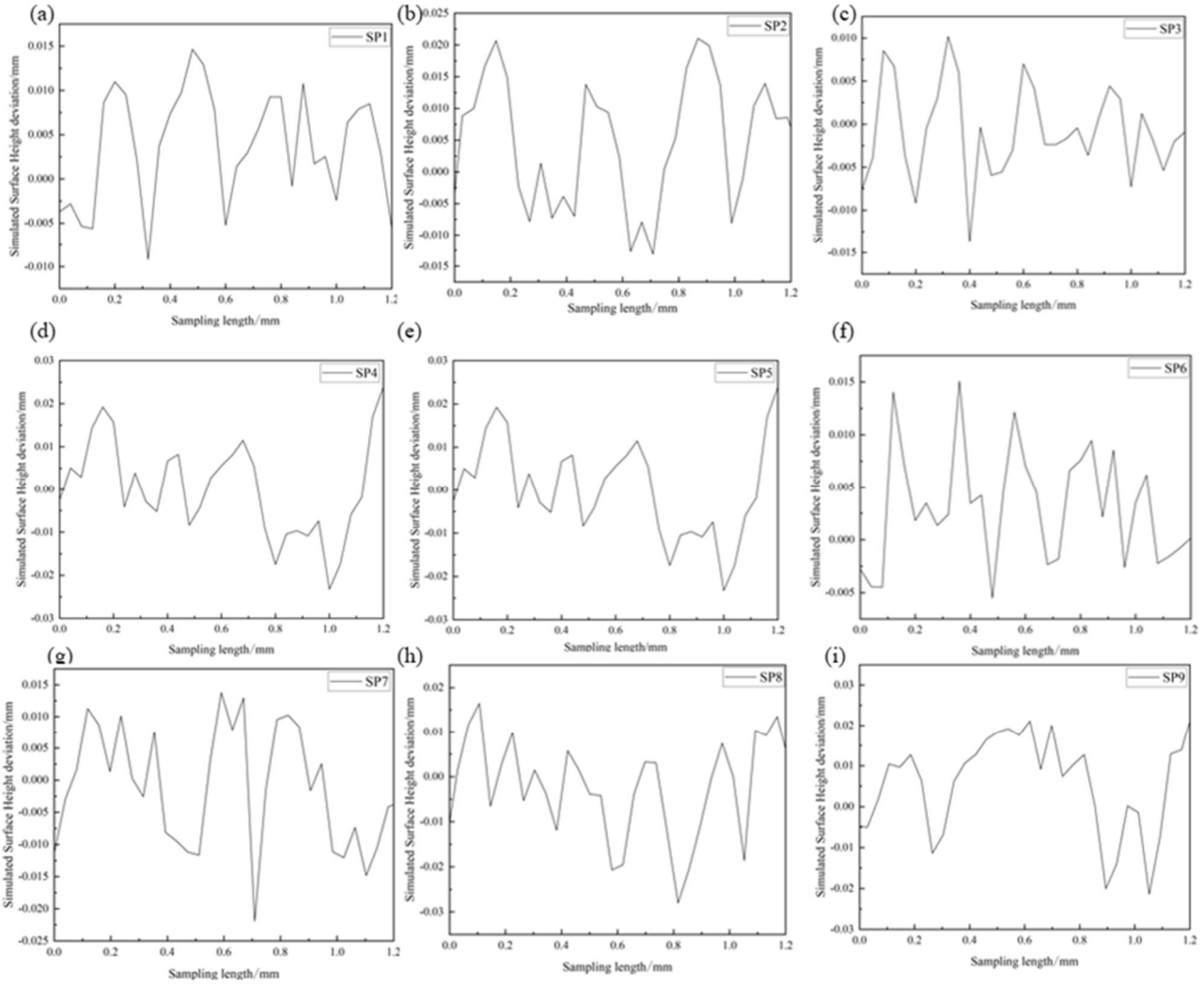

Fig. 6 *Surface roughness profile graph; Test Group Number: (a)Test 1, (b)Test 2, (c)Test 3, (d)Test 4, (e)Test 5, (f)Test 6, (g)Test 7, (h)Test 8, (i)Test 9*

After 9 sets of shot peening simulations, the surface roughness under different conditions are compared. Fig. 5 and Fig. 6 show the surface roughness morphology after shot peening. This may be that the normal component of the projectile velocity is relatively small when the angle of incidence is large, resulting in small impact force and shallow craters. Combined with Fig. 6, it can be seen that the higher the tangential velocity of the projectile, the greater the impact force on the surface. Consequently, the surface roughness becomes small. When the incidence angle is small, the impact force will increase. As a result, the material surface or even the underlying layer may develop cracks, leading to severe damage to the material surface.

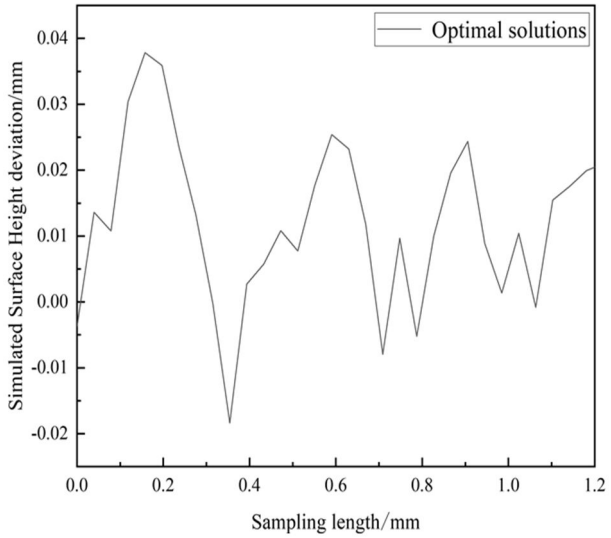

Fig. 7 *Optimal combination of solutions*

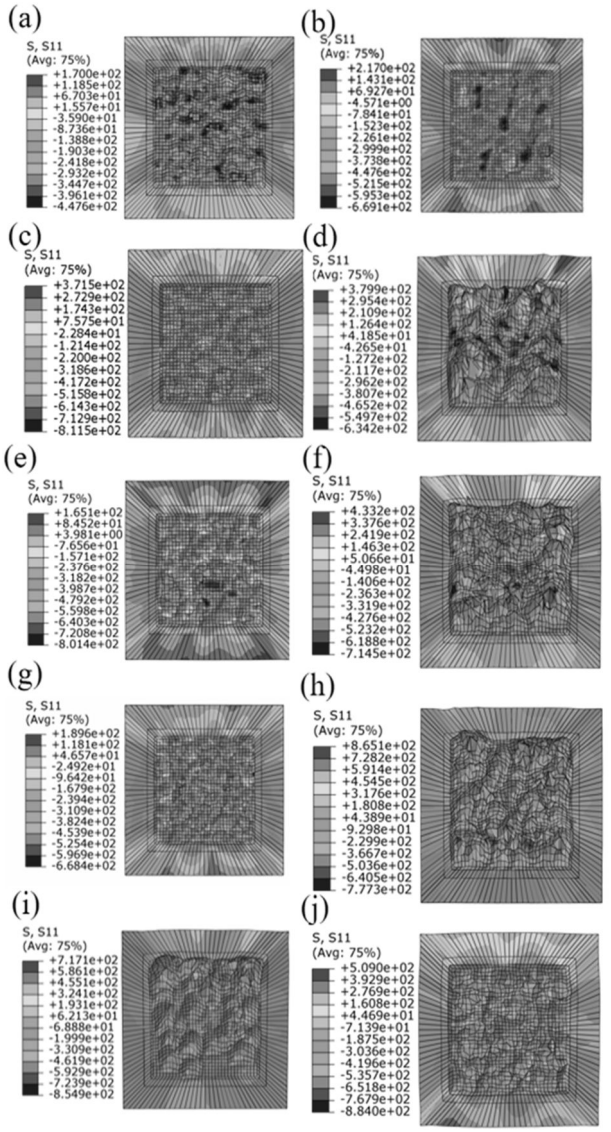

Fig. 8 *Residual stress diagram; Test Group Number: (a)Test 1, (b)Test 2, (c)Test 3, (d)Test 4, (e)Test 5, (f)Test 6, (g)Test 7, (h)Test 8, (i)Test 9 (j) Optimal combination of solutions*

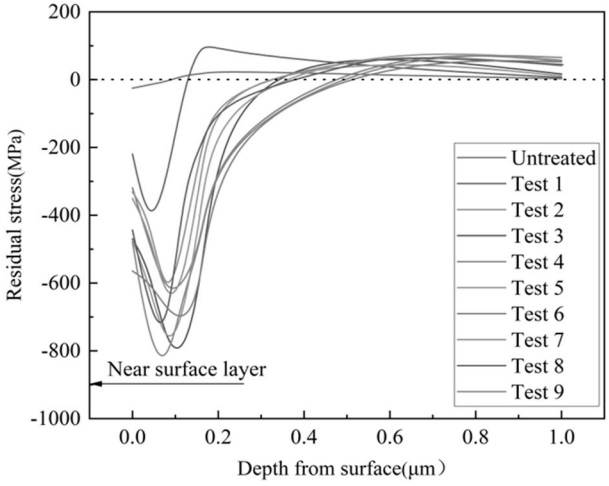

Fig. 9 *Residual stress diagram for shot peening test simulation; Test Group Number: (a)Test 1, (b)Test 3, (c)Test 4, (d)Test 5, (e)Test 6, (f) Test 7, (g)Test 8, (h)Test 9, (i) Optimal combination of solutions*

After experimental operation and data analysis, the optimal roughness profile curve is selected from 9 groups of results, as shown in Fig. 7. This profile is of great significance to improve the material performance, ensure the surface finish, and reduce the friction loss and stress concentration.

Corresponding residual stress plots for different shot peening parameters are shown in Fig. 8, and the residual stress profiles are shown in Fig. 9. From these two plots, it can be seen that when the shot peening parameters change, the maximum residual compressive stress, the depth of the residual compressive stress layer, and the residual compressive stress on the surface increase to a certain extent. As the diameter of the projectile increases, the depth of the maximum residual compressive stress does not change significantly, with continuous increase. This may be that when the diameter of the projectile is large, its contact range with the target material expands and absorbs more energy, resulting in an increase in the depth of the residual compressive stress. In addition, the increase in projectile diameter may lead to a strong impact force, which is also a factor contributing to the sustained increase in the maximum compressive residual stress [24-25].

The orthogonal table L_9 (3^3) is constructed based on the 3-factor, 3-level orthogonal test methodology. Using he GUI user interface to generate scrip files, and running them in the finite element analysis software MATLAB, the post-processing of shot peening simulation is analyzed to obtain the roughness of the target material surface crater along the horizontal direction, as well as the residual stress along the depth direction of the projectile group impact. The variation curves of the residual stress with depth direction are drawn respectively. The residual compressive stress on the surface σ_s, the depth of the residual compressive

stress layer d_0, and the maximum value of the residual compressive stress σ_m are collected. The orthogonal test table L_9 (3^3) and the simulation results data are shown in Tab. 4 [26].

Tab. 4 *Orthogonal trials with composite scores*

Test No.	Settings of different shot peening parameter levels			Assessment indicators			Evaluation mark
	A (m.s^{-1})	B (mm)	C (°)	σs	d0	σm	
1	60	0.3	45	-219.604	0.127	-447.605	16.683
2	60	0.4	60	-331.467	0.246	-674.595	25.158
3	60	0.5	90	-469.941	0.423	-811.52	32.047
4	80	0.3	60	-319.307	0.449	-634.743	23.862
5	80	0.4	90	-473.028	0.319	-801.483	31.871
6	80	0.5	45	-564.845	0.495	-714.545	31.997
7	100	0.3	90	-350.708	0.203	-668.423	25.483
8	100	0.4	45	-443.829	0.375	-777.329	30.538
9	100	0.5	60	-479.236	0.436	-854.917	33.365

6.3 Analysis of data results

In the simulation, due to the inconsistency of the quantitative values of the three targets, the three indicators for evaluating the effectiveness of shot peening data cannot be superimposed. Here, the orthogonal test results processing method using a percentage system weighted composite score is adopted. Eq. (2) shows the calculation formula for the weighted composite average value Y. The weighting coefficients Ci (i = 1, 2, 3) are determined in accordance with the significance of each target in the shot peening effect. For the surface residual compressive stress X1(σs), the depth of the residual compressive stress layer X2(d0), and the maximum residual compressive stress value X3(σm), the weighting factor values are set at 25%, namely, C1 = 25%, C2 = 25%, C3 = 25%.

$$X = C_1X_1 + C_2X_2 + C_3X_3 \tag{2}$$

The interrelationship between the variables and the evaluation of the composite indexes are explored to identify the optimal combination of process parameters and achieve the most favorable shot peening results. Consequently, the polar analysis method is used to analyze the result data derived from the orthogonal test. The underlying principle is shown in Fig. 10.

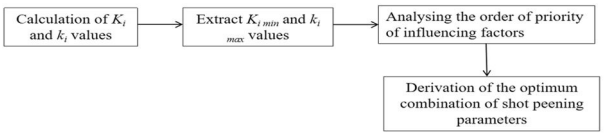

Fig. 10 *A schematic diagram of the extreme variance analysis of the shot peening test*

In the process of analyzing extreme differences in the orthogonal test results, it is recommended to choose the results of the four indicators output by ABAQUS under each parameter combination scheme as evaluation indicators [27]. This will be able to determine the primary and secondary relationships of each factor, as well as the formula for calculating the extreme effects of shot peening parameters.

$$\begin{cases} \Delta j = \left| k_{ij\,\max} - k_{ij\,\min} \right| \\ k_{ij} = K_{ij} / 3 \end{cases} \tag{3}$$

Where:

i…The levels of each factor in Tab. 4, where *i* = 1, 2, 3;

j…The codes of each factor in Tab. 5, where *j* = 1, 2, 3;

K_i…The evaluation index;

K_{ij}…The average value of the evaluation index.

According to Eq. (3), in a set of data, the difference between the maximum value of the test indicator and the minimum value is considered. The influence of different blasting process parameters on the peening effect can be measured by the magnitude of this difference. When the difference is small, the effect is relatively weak. Conversely, if the difference is large, it indicates that the factor has a significant impact on the shot peening effect. The level combinations of the three factors that can yield optimal values can be determined through extreme variance analysis.

As shown in Tab. 5, the optimal combination of shot peening parameters for 7B50 aluminium alloy shot peening process is $A_3B_3C_3$ based on the comprehensive evaluation of the extreme difference value. That is, the impact speed is taken as 100 m.s^{-1}, the diameter of the projectile as 0.5 mm, the impact angel as 90°, and the projectile as the cast steel shot.

The depth of the residual compressive stress layer, the surface residual compressive stress value σs, and the maximum residual compressive stress value σm are three evaluation indicators. Based on the above analysis of extreme deviation, the factors in Tab. 4 can be used to determine the primary and secondary relationships of the influence of the shot peening effect on the depth of the residual compressive stress layer, the surface residual compressive stress value, and the maximum residual stress value [28].

Tab. 5 *Extreme variance analysis results for shot peening effectiveness*

Working conditions (K_j)	A	B	C
K_1	73.888	66.028	79.218
K_2	87.73	87.567	82.385
K_3	89.386	97.409	89.401
k_1	24.629	22.009	26.406
k_2	29.243	29.189	27.462
k_3	29.795	32.47	29.8
Extremely poor	5.166	10.461	3.394
Order of priority		B > A > C	
Optimum level	A_3	B_3	C_3
Optimum combination of shot peening parameters		$A_3B_3C_3$	

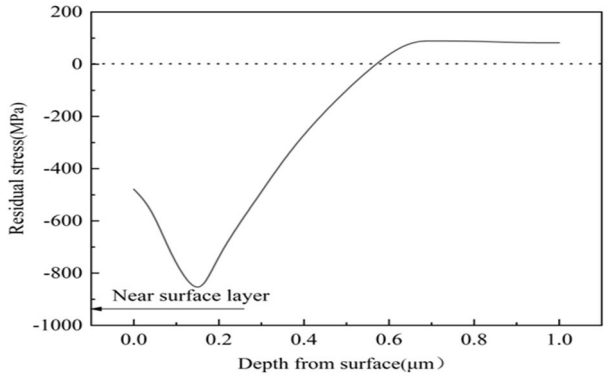

Fig. 11 *Residual stress curves for the combination of optimal solutions*

The simulation model based on the residual stress theory [29] can comprehensively and systematically obtain the residual stress distribution generated by shot peening. Based on this, the residual stress values derived from the simulation are more consistent with the actual situation and are more realistic and reliable. The simulation is conducted using the optimal combination of process parameters, and the results are shown in Fig.11. At this time, σ_s = -478.728MPa, d_0 = 0.533, σ_m =-884.023MPa and the combined score value is 34.082. Based on the analysis of the extreme difference values of the four evaluation indicators, it can be determined that the optimal level combination of each factor is $A_3B_3C_3$. This combination corresponds to the highest comprehensive score of the optimal process parameter combination scheme and can be regarded as the optimal process parameter combination for the shot peening parameter treatment of 7B50 aluminium alloy [30]. Through this analysis, a more accurate and suitable parameter configuration is identified for the specific treatment of this alloy, providing valuable guidance for practical applications in this field.

7 Conclusions

The secondary development of Python within ABAQUS is presented here. The parameters of the Python script file are directly modified in the GUI user interface. Subsequently, the task is submitted and analyzed in the ABAQUS solver. The modeling and post-processing analysis of shot peening parameters can be accomplished only by changing the parameters, avoiding the possible errors that may occur manually. Moreover, the established random shot peening model employs the orthogonal test method to design experiments on the process parameters affecting shot peening. This is accomplished by using simulation algorithms and comprehensive judgment processing of the data, which leads to the significance ranking of the influence of the three shot peening parameters on the shot peening effect. In addition, an optimal combination of shot peening parameter schemes is determined to reduce the time for experiment and provide convenience and reference for the study of shot blasting.

- (1) Through a thorough analysis, it is found that the shot peening parameters and their value ranges are determined. Eventually, the optimal combination of process parameters, namely A3B3C3, is obtained. The specific values are an impact speed of 100 $m.s^{-1}$, a projectile diameter of 0.5mm, and an impact angle of 90°;
- (2) Based on extreme difference values, it can be seen that the three influencing parameters on the shot peening parameter are: B > A > C; in the descending order of intensity, they are impact speed, pellet size, and impact angle;

- (3) The surface properties of 7B50 aluminium alloy targets can be enhanced by adjusting the shot peening parameters. The addition of many other factors to shot peening can play a leading role in making the surface integrity more comprehensive and informative.

Acknowledgement

This work was supported by the Natural Science Foundation of Anhui Province of China (2208085QE154) and the Research Initiation Fund Project of Anhui Polytechnic University (2021YQQ001).

Author Contributions

Anheng Wang: Supervision, Writing – Review & Editing. Shangqi Duan: Writing – Original Draft, Conceptualization, Software, Methodology. Wei Zhang: Writing – Review & Editing, Funding acquisition. Fan Li: Formal analysis, Visualization.

Data availability statement

The data cannot be made publicly available upon publication because no suitable repository exists for hosting data in this field of study. The data that support the findings of this study are available upon reasonable request from the authors.

Conflicts of interest

The authors declare that they have no involvement in any organization or entity with any financial interest.

Reference

[1] HAN, X., ZHANG, Z., WANG, B., THRUSH, S. J., BARBER, G. C., & QIU, F. (2022). Microstructures, compressive residual stress, friction behavior, and wear mechanism of quenched and tempered shot peened medium carbon steel. *Wear*, Vol. 488-489, pp. 204131. https://doi.org/10.1016/j.wear.2021.204131

[2] RAGHUVARAN, P., SURESH, M., NARASIMHARAJ, V., & RAJESH, A. (2023). Enhancing the fatigue strength of stir-casted Al7075-SiC composites through heat treatment and shot peening. *Physica Scripta*, Vol. 98, No. 10, pp. 105915. DOI: 10.1088/1402-4896/acf3b7

[3] JAMBOR, M., TRŠKO, L., ŠULÁK, I., ŠIŠKA, F., BAGHERIFARD, S., GUAGLIANO, M., & FLORKOVÁ, Z. (2024). Application of shot peening to improve fatigue properties via enhancement of precipitation response in high-strength Al–Cu–Li alloys. Journal of Materials Research and Technology, Vol. 33, pp. 9595-9602. https://doi.org/10.1016/j.jmrt.2024.11.260

[4] LIN, Q., WEI, P., LIU, H., ZHU, J., ZHU, C., & WU, J. (2022). A CFD-FEM numerical study on shot peening. *International Journal of Mechanical Sciences*, Vol. 223, pp. 107259. https://doi.org/10.1016/j.ijmecsci.2022.107259

[5] XIE, L., ZHANG, J., XIONG, C., WU, L., JIANG, C., & LU, W. (2012). Investigation on experiments and numerical modelling of the residual stress distribution in deformed surface layer of Ti–6Al–4V after shot peening. *Materials & Design*, Vol. 41, pp. 314-318. https://doi.org/10.1016/j.matdes.2012.05.024

[6] ZHANG, Y., LAI, F., QU, S., JI, V., LIU, H., & LI, X. (2020). Effect of shot peening on residual stress distribution and tribological behaviors of 17Cr2Ni2MoVNb steel. *Surface and Coatings Technology*, Vol. 386, pp. 125497. https://doi.org/10.1016/j.surfcoat.2020.125497

[7] GARIÉPY, A., BRIDIER, F., HOSEINI, M., BOCHER, P., PERRON, C., & LÉVESQUE, M. (2013). Experimental and numerical investigation of material heterogeneity in shot peened aluminium alloy AA2024-T351. *Surface and Coatings Technology*, Vol. 219, pp. 15-30. https://doi.org/10.1016/j.surfcoat.2012.12.046

[8] WU, J., LIU, H., WEI, P., LIN, Q., & ZHOU, S. (2020). Effect of shot peening coverage on residual stress and surface roughness of 18CrNiMo7-6 steel. *International Journal of Mechanical Sciences*, Vol. 183, pp. 105785. https://doi.org/10.1016/j.ijmecsci.2020.105785

[9] ALI, A., AN, X., RODOPOULOS, C. A., BROWN, M. W., O'HARA, P., LEVERS, A., & GARDINER, S. (2007). The effect of controlled shot peening on the fatigue behaviour of 2024-T3 aluminium friction stir welds. *International Journal of Fatigue*, Vol. 29, No. 8, pp. 1531-1545. https://doi.org/10.1016/j.ijfatigue.2006.10.032

[10] ZHANG, X., WEI, D., LIU, X., XIAO, J., & YANG, S. (2025). Effect of compressive residual stress and surface morphology introduced by shot peening on the improvement of fretting fatigue life of TC4. International Journal of

Fatigue, Vol. 194, pp. 108835. https://doi.org/10.1016/j.ijfatigue.2025.108835

[11] KE, J., HE, J., WU, Z., & XIANG, Z. (2023). Fatigue reliability design of composite helical spring with nonlinear stiffness based on ply scheme design. *Composite Structures*, Vol. 319, pp. 117119. https://doi.org/10.1016/j.compstruct.2023.117119

[12] GAO, S., YANG, J., XU, Y., ZHANG, Y., & BAI, Q. (2024). Effect of dynamic constitutive differences in materials on the impact performance of CFST via secondary development of ABAQUS. *Structures*, Vol. 62, pp. 106236. https://doi.org/10.1016/j.istruc.2024.106236

[13] QIANG, X., DUAN, X., JIANG, X., & LU, Q. (2024). Python-based numerical study on bolted joints between Fe-SMA and steel plates for structural reinforcements. *Structures*, Vol. 69, pp. 107316. https://doi.org/10.1016/j.istruc.2024.107316

[14] ZHANG, P., GAO, Y., YUE, X., SUN, Y., ZHOU, H., & ZHANG, J. (2024). Study on the fatigue performance and Residual Stress of subsurface fluid flow of 2519a aluminum alloy based on water jet peening. *Vacuum*, Vol. 230, pp. 113648. https://doi.org/10.1016/j.vacuum.2024.113648

[15] LI, C., & CHEN, S. (2023). The effect of chipbreaker parameters on the cutting temperature of Inconel 718 alloy based on the secondary development of Abaqus. *Journal of Physics: Conference Series*, Vol. 2541, No. 1, pp. 012043. DOI: 10.1088/1742-6596/2541/1/012043

[16] PREMA, V., & UMA RAO, K. (2018). Interactive graphical user interface (GUI) for wind speed prediction using wavelet and artificial neural network. *Journal of the Institution of Engineers (India): Series B*, Vol. 99, pp. 467-477. https://doi.org/10.1007/s40031-018-0339-3

[17] OOSTROM, M. T., COLBY, S. M., & METZ, T. O. (2024). DEIMoS GUI: An Open-Source User Interface for a High-Dimensional Mass Spectrometry Data Processing Tool. *Journal of Chemical Information and Modeling*, Vol. 64, No. 5, pp. 1419-1424. https://doi.org/10.1021/acs.jcim.3c01222

[18] DODO, Y., ARIF, K., ALYAMI, M., ALI, M., NAJEH, T., & GAMIL, Y. (2024). Estimation of compressive strength of waste concrete utilizing fly ash/slag in concrete with interpretable approaches: optimization and graphical user interface (GUI). *Scientific Reports*, Vol. 14, No. 1, pp. 4598. https://doi.org/10.1038/s41598-024-54513-y

[19] LIU, Y. G., LI, H. M., & LI, M. Q. (2020). Roles for shot dimension, air pressure and duration in the fabrication of nanocrystalline surface layer in TC17 alloy via high energy shot peening. *Journal of Manufacturing Processes*, Vol. 56, No. Part A, pp. 562-570. https://doi.org/10.1016/j.jmapro.2020.05.019

[20] CAO, Y., NIU, T., GAI, P., CHEN, Y., PANG, J., & XU, W. (2023). Numerical simulation for investigating the impact of shot peening process parameters via surface reconstruction. *The International Journal of Advanced Manufacturing Technology*, Vol. 129, No. 5, pp. 2721-2734. https://doi.org/10.1007/s00170-023-12423-9

[21] JIANG, S., GAO, M., WANG, J., LIU, J., FENG, H., & XU, X. (2024). Analysis and multi-objective optimization design of sinusoidal DSEM with two different excitation modes based on Gray-Fuzzy-Taguchi method. *Computers and Electrical Engineering*, Vol. 117, pp. 109251. https://doi.org/10.1016/j.compeleceng.2024.109251

[22] MAMOŃ, F., JASKEVIČ, M., MAREŠ, J., NOVOTNÝ, J. (2023). Fire Resistance Test of Geopolymer Coatings on Non-Metallic Underlying Substrates. *Manufacturing Technology*, Vol. 23, No. 2, pp. 225-232. DOI: 10.21062/mft.2023.026

[23] YAO, S. L., WANG, G. Y., YU, H., WANG, J., LI, K. S., LIU, S., TU, S. T. (2022). Influence of submerged micro-abrasive waterjet peening on surface integrity and fatigue performance of TA19 titanium alloy. *International Journal of Fatigue*, Vol. 164, pp. 107076. https://doi.org/10.1016/j.ijfatigue.2022.107076

[24] ZHAO, J., TANG, J., ZHOU, W., JIANG, T., & LIU, H. (2023). Comprehensive experimental study of shot peening on the surface integrity evolution of 12Cr2Ni4A high-strength steel. *The International Journal of Advanced Manufacturing Technology*, Vol. 124, No. 1, pp. 143-164. https://doi.org/10.1007/s00170-022-10458-y

[25] ZHANG, S., LENG, Z., GU, H., YIN, J., WANG, Z., & LIU, Y. (2022). Simulation and experiment research on the surface deformation and residual stress of fractal rough surface single-shot peening. *Applied Sciences*, Vol. 12, No. 14, pp. 6891. https://doi.org/10.3390/app12146891

[26] MA, Z., CHEN, T., WANG, Z., XING, X., HOU, X., & CHANG, C. (2023). Analysis of residual stress of gear tooth root after shot peening process. *The International Journal of Advanced Manufacturing Technology*, Vol. 125, No. 5, pp. 2147-2160. https://doi.org/10.1007/s00170-023-10875-7

[27] GIULIANO, G., PARODO, G., POLINI, W., SORRENTINO, L. (2023). Cold Blow Forming of a Thin Sheet in AA8006 Aluminum Alloy. *Manufacturing Technology*. Vol. 23, No. 3, pp. 284-289. DOI: 10.21062/mft.2023.038

[28] ROSHITH, P. (2024). The influence of compressive residual stress on metallurgical and mechanical properties of materials exposed to shot peening: a review. *Canadian Metallurgical Quarterly*, Vol. 63, No. 2, pp. 373-413. https://doi.org/10.1080/00084433.2023.2213045

[29] DONG, X., DUAN, X. (2005). The Research of Continuous Water Jet Critical Shot Peening Pressure. *Proceedings of the International Conference on Mechanical Engineering and Mechanics*, Vol. 2, pp.26-28.

[30] CHOCHLÍKOVÁ, H., MAJERÍK, J., BARÉNYI, I., GAVALEC, M., ESCHEROVÁ, J., PECANAC, M., ET AL. (2024) Research on FSW Welds of Al-Alloy Modified by Laser Shock Peening Process. *Manufacturing Technology*, Vol. 24, No. 1, pp. 53-61. DOI: 10.21062/mft.2024.018